THE CURIOUS CASE OF BENIGN MEMORIZATION

Anonymous authors
Paper under double-blind review

ABSTRACT

Despite the empirical advances of deep learning across a variety of learning tasks, our theoretical understanding of its success is still very restricted. One of the key challenges is the overparametrized nature of modern models, enabling complete overfitting of the data even if the labels are randomized, i.e. networks can completely *memorize* all given patterns. While such a memorization capacity seems worrisome, in this work we show that under training protocols that include *data augmentation*, neural networks learn to memorize entirely random labels in a benign way, i.e. they learn embeddings that lead to highly non-trivial performance under nearest neighbour probing. We demonstrate that deep models have the surprising ability to separate noise from signal by distributing the task of memorization and feature learning to different layers. As a result, only the very last layers are used for memorization, while preceding layers encode performant features which remain largely unaffected by the label noise. We explore the intricate role of the augmentations used for training and identify a memorization-generalization trade-off in terms of their diversity, marking a clear distinction to all previous works. Finally, we give a first explanation for the emergence of benign memorization by showing that *malign* memorization under data augmentation is infeasible due to the insufficient capacity of the model for the increased sample size. As a consequence, the network is forced to leverage the correlated nature of the augmentations and as a result learns meaningful features. To complete the picture, a better theory of feature learning in deep neural networks is required to fully understand the origins of this phenomenon.

1 INTRODUCTION

Deep learning has made tremendous advances in the past decade, leading to state-of-the-art performance on various learning tasks such as computer vision (He et al., 2016), natural language processing (Devlin et al., 2019) and graph learning (Kipf & Welling, 2017). While some progress has been made regarding the theoretical understanding of these deep models (Arora et al., 2018; Bartlett et al., 2019; 2017; Neyshabur et al., 2015; 2018; Dziugaite & Roy, 2017), the considered settings are unfortunately often very restrictive and the insights made are only qualitative or very loose. One of the key technical hurdles hindering progress is the highly overparametrized nature of neural networks employed in practice, which is in stark contrast with classical learning theory, according to which *simpler hypotheses compatible with the data* should be preferred. The challenge of overparametrization is beautifully illustrated in the seminal paper of Zhang et al. (2017), showing that deep networks are able to fit arbitrary labelings of the data, i.e. they can completely *memorize* all the patterns. This observation renders tools from classical learning theory such as VC-dimension or Rademacher complexity vacuous and commands new avenues to be investigated. The random label experiment has been applied3 as a sanity check for new techniques (Arora et al., 2018; 2019a; Bartlett et al., 2017; Dziugaite & Roy, 2017), where an approach is evaluated based on its ability to distinguish between networks that memorize or truly learn the data. From a classical perspective, memorization is thus considered as a bug, not a feature, and goes hand in hand with bad generalization.

In this work we challenge this view by revisiting the randomization experiment of Zhang et al. (2017) with a slight twist: we change the training protocol by adding *data augmentation*, a standard practice used in almost all modern deep learning pipelines. We show that in this more practical setting, the story is more intricate;

Neural networks trained on random labels with data augmentation learn useful features!

More precisely, we show that probing the embedding space with the nearest neighbour algorithm of such a randomly trained network admits highly non-trivial performance on a variety of standard benchmark datasets. Moreover, such networks have the surprising ability to separate signal from noise, as all layers except for the last ones focus on feature learning while not fitting the random labels at all. On the other hand, the network uses its last layers to learn the random labeling, at the cost of clean accuracy, which strongly deteriorates. This is further evidence of a strong, implicit bias present in modern models, allowing them to learn performant features even in the setting of complete noise. Inspired by the line of works on benign overfitting (Bartlett et al., 2020; Sanyal et al., 2021; Frei et al., 2022), we coin this phenomenon *benign memorization*. We study our findings through the lens of capacity and show that under data augmentation, modern networks are forced to leverage the correlations present in the data to achieve memorization. As a consequence, the model learns invariant features which have been identified to have strong discriminatory power in the field of self-supervised learning (Caron et al., 2021; Grill et al., 2020; Bardes et al., 2022; Zbontar et al.; Chen & He, 2021). Specifically, we make the following contributions:

- We make the surprising observation that learning under complete label noise still leads to highly useful features (*benign memorization*), showing that memorization and generalization are not necessarily at odds.
- We show that deep neural networks exhibit an astonishing capability to separate noise and signal between different layers, fitting the random labels only at the very last layers.
- We highlight the intricate role of augmentations and their interplay with the capacity of the model class, forcing the network to learn the correlation structure.
- We interpret our findings in terms of invariance learning, an objective that has instigated large successes in the field of self-supervised learning.

2 Related Work

Memorization. Our work builds upon the seminal paper of Zhang et al. (2017) which showed how neural networks can easily memorize completely random labels. This observation has inspired a multitude of follow-up works and the introduced randomization test has become a standard tool to assess the validity of generalization bounds (Arora et al., 2018; 2019a; Bartlett et al., 2017; Dziugaite & Roy, 2017). The intriguing capability of neural networks to simply memorize data has inspired researchers to further dissect the phenomenon, especially in the setting where only a subset of the targets is randomized. Arpit et al. (2017) studies how neural networks tend to learn shared patterns first, before resorting to memorization when given real data, opposed to random labels where examples are fitted independently. Feldman & Zhang (2020) study the setting when real but "long-tailed" data is used and show how memorization in this case can be beneficial to performance. Maennel et al. (2020); Pondenkandath et al. (2018) on the other hand show how pre-training networks on random labels can sometimes lead to faster, subsequent training on the clean data or novel tasks. Finally, Zhang et al. (2021) show how training on random labels can be valuable for neural architecture search. In all these previous works, data augmentation is excluded from the training pipeline. For partial label noise, it is well-known in the literature that neural networks exhibit surprising robustness (Rolnick et al., 2017; Song et al., 2020; Patrini et al., 2017) and generalization is possible. We highlight however that this setting is distinct from *complete* label noise, which we study in this work.

Data augmentation. Being a prominent component of deep learning applications, the benefits of data augmentation have been investigated theoretically in the setting of clean labels (Chen et al., 2020b; Dao et al., 2019; Wu et al., 2020; Hanin & Sun, 2021). The benefits of data augmentation have been verified empirically when only a subset of the data is corrupted (Nishi et al., 2021). On the other hand, investigations with pure label noise where no signal remains in the dataset are absent in the literature. Finally, we want to highlight the pivotal role of data augmentation in self-supervised learning frameworks (Caron et al., 2021; Grill et al., 2020; Bardes et al., 2022; Zbontar et al.; Chen & He, 2021), where it facilitates learning of invariant features.

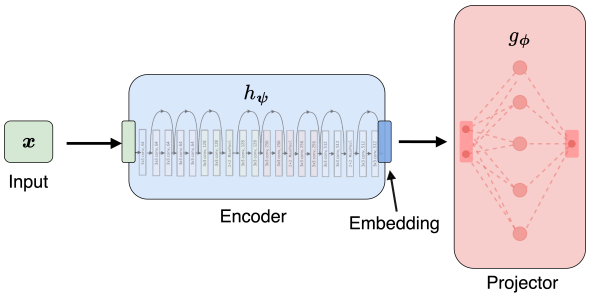

(a) Visualization of an encoder-projector pair. The encoder is typically chosen as a *ResNet18*, while the projector is a one hidden-layer MLP.

(b) Illustration of standard data augmentation. Notice how each augmentation indeed preserves the label "cat".

Figure 1: (Left) Encoder-projector pair. (Right) Standard data augmentations.

3 Background

Setting. In this work we consider the standard classification setting, where we are given $n \in \mathbb{N}$ i.i.d. samples $(\boldsymbol{x}_1, \boldsymbol{y}_1), \ldots, (\boldsymbol{x}_n, \boldsymbol{y}_n) \overset{i.i.d.}{\sim} \mathcal{D}$ from some data distribution $\mathcal{D}$, consisting of inputs $\boldsymbol{x} \in \mathbb{R}^d$ and one-hot targets $\boldsymbol{y} \in \mathbb{R}^C$, each encoding one out of C classes. We consider a family of parametrized functions (in this work, neural networks) $f_{\boldsymbol{\theta}} : \mathbb{R}^d \to \mathbb{R}^C$, where $\boldsymbol{\theta} \in \Theta$ denotes the (concatenated) weights from some space $\Theta \subseteq \mathbb{R}^p$ where p is the total number of parameters. Moreover, we specify a loss function $l : \mathbb{R}^C \times \mathbb{R}^C \to \mathbb{R}_+$ which measures the discrepancy between a prediction $f_{\boldsymbol{\theta}}(\boldsymbol{x})$ and its corresponding target $\boldsymbol{y}$, i.e. $l(f_{\boldsymbol{\theta}}(\boldsymbol{x}), \boldsymbol{y})$. We then perform learning by minimizing the empirical loss $\hat{L}$ as a function of the parameters $\boldsymbol{\theta}$,

$$\hat{\boldsymbol{\theta}} := \text{argmin}_{\boldsymbol{\theta} \in \Theta} \hat{L}(\boldsymbol{\theta}) := \text{argmin}_{\boldsymbol{\theta} \in \Theta} \sum_{i=1}^{n} l(f_{\boldsymbol{\theta}}(\boldsymbol{x}_i), \boldsymbol{y}_i) \tag{1}$$

using some form of stochastic gradient descent and measure the resulting generalization error $L(\hat{\boldsymbol{\theta}}) = \mathbb{E}_{(\boldsymbol{x},\boldsymbol{y}) \sim \mathcal{D}} \left[l(f_{\hat{\boldsymbol{\theta}}}(\boldsymbol{x}), \boldsymbol{y}) \right]$. We denote by $p_{\boldsymbol{X}}$ the marginal density of the inputs and by $p_{\boldsymbol{Y}|\boldsymbol{X}}$ the conditional density of the labels given an input. $p_{\boldsymbol{Y}|\boldsymbol{X}}$ encodes the statistical relationship between an input $\boldsymbol{x}$ and the associated label $\boldsymbol{y}$. As typical in practice, we assume that we are in the so-called interpolation regime (Ma et al., 2018), i.e. we assume that stochastic gradient descent can find a parameter configuration $\hat{\boldsymbol{\theta}}$ that achieves zero training loss (see Eq. 1).

Architecture. Throughout this work, we consider networks composed of an encoder $h_{\boldsymbol{\psi}} : \mathbb{R}^d \to \mathbb{R}^m$ and a projector $g_{\boldsymbol{\phi}} : \mathbb{R}^m \to \mathbb{R}^C$, where both $\boldsymbol{\psi}$ and $\boldsymbol{\phi}$ denote the parameters of the respective building block. As an encoder, we typically employ modern convolutional architectures such as *ResNets* (He et al., 2016) or *VGG* (Simonyan & Zisserman, 2014), excluding the final fully-connected layers, while the projector is usually an MLP with one hidden layer. We illustrate such a network in Fig. 1a. Such architectures have become very popular in the domain of feature learning and are extensively used in unsupervised and self-supervised learning (Caron et al., 2021; Grill et al., 2020; Bardes et al., 2022; Zbontar et al.). In this work, we are interested in assessing the quality of the encoder's features $h_{\boldsymbol{\psi}}$ when the network $f_{\boldsymbol{\theta}} = g_{\boldsymbol{\phi}} \circ h_{\boldsymbol{\psi}}$ is trained on random labels.

Probing. To evaluate the embeddings $h_{\boldsymbol{\psi}}$, we apply nearest-neighbour-based *probing*, which refers to performing K-nearest-neighbour classification based on the embeddings $\{(h_{\boldsymbol{\psi}}(\boldsymbol{x}_i), \boldsymbol{y}_i)\}_{i=1}^n$. We fix the number of neighbours to $K = 20$ throughout this work unless otherwise specified. Probing measures how useful a given set of features $h_{\boldsymbol{\psi}}$ is for a fixed task. A special case we will often consider in this work is probing the encoder of a network at initialization, which we refer to as probing at initialization. Due to the very restricted complexity of probing, the resulting performance is very dependent on the quality of the input representations $h_{\boldsymbol{\psi}}$. Such method has been used to assess the quality of a given embedding space in various works, for instance Alain & Bengio (2017); Chen et al. (2020a); Caron et al. (2021); Grill et al. (2020); Bardes et al. (2022); Zbontar et al..

Random labels and memorization. Denote by $\boldsymbol{e}_l \in \mathbb{R}^C$ the l-th unit vector, i.e. the one-hot encoding of class l. Zhang et al. (2017) introduced a randomization test, where any clean label

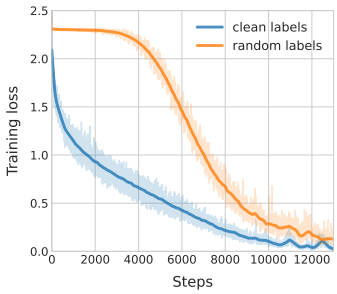

Figure 2: Fitting random labels on unaugmented data on *CIFAR10* with a *ResNet18* is not significantly slower than fitting clean labels.

Layer	Initialization	End of training
Layer 1	36.9	34.3
Layer 2	36.4	33.5
Layer 3	36.5	30.4
Layer 4	36.2	14.9
Embedding	40.2	12.4
Projector hidden layer	38.4	10.5
Output	24.2	10.5

Table 1: K-NN probing accuracies (percentage) for a *ResNet18* at initialization versus at the end of training on random labels without augmentations on *CIFAR10*. The four layers correspond to the intermediate representations after each stage of a *ResNet*.

$\boldsymbol{y}_i \in \{\boldsymbol{e}_1, \dots, \boldsymbol{e}_C\}$ in the training set is replaced by a random one-hot encoding, $\tilde{\boldsymbol{y}}_i = \boldsymbol{e}_l$ where $l \sim \mathcal{U}(\{1, \dots, C\})$ with $\mathcal{U}$ denoting the uniform distribution over the discrete set $\{1, \dots, C\}$. Throughout this text, we will denote randomized variables with $\sim$ on top. Notice that such an intervention destroys any statistical relationship between inputs and targets, i.e. $p_{\boldsymbol{Y}|\boldsymbol{X}} = p_{\boldsymbol{Y}}$. As a consequence, training on such a dataset should become very difficult as there is no common pattern left to exploit and an algorithm has to resort to a pure memorization approach. Zhang et al. (2017) showed that deep neural networks have an astonishing capacity to perform such memorization tasks, easily overfitting any random label assignment even on large-scale datasets such as *ImageNet* (Deng et al., 2009) without a large increase in training time (see Fig. 2). Even explicit regularizers such as weight decay and *Dropout* (Srivastava et al., 2014) can be used in a standard manner, data augmentation however is excluded from the pipeline. We have reproduced a subset of the results of Zhang et al. (2017) in Table 2, first column. As expected, deep neural networks indeed manage to achieve zero training error across a variety of datasets while not generalizing at all, both with respect to a random test labeling as well as the original, clean test labels. In order to further study the amount of distortion in the resulting embedding space, we apply nearest-neighbour probing with respect to the clean data. More precisely, given the features $h_{\boldsymbol{\psi}}$ learnt from training on the random label task $\{(\boldsymbol{x}_i, \tilde{\boldsymbol{y}}_i)\}_{i=1}^n$, we apply probing based on the clean training data $\{(\boldsymbol{x}_i, \boldsymbol{y}_i)\}_{i=1}^n$ and evaluate with respect to clean test data. We display the results in Table 1. In line with previous works, (Cohen et al., 2018; Maennel et al., 2020), we find that while very early layers might retain their performance at initialization, a significant drop occurs with increasing depth, further highlighting the lack of feature learning and the *malignant* nature of memorization in this setting.

Data Augmentation. A standard technique present in almost all computer vision pipelines is data augmentation. We consider transformations $T : \mathbb{R}^d \to \mathbb{R}^d$, that take a given input $\boldsymbol{x}$ and produce a new augmentation $\bar{\boldsymbol{x}} := T(\boldsymbol{x})$, which by design, should preserve the associated label, i.e. $\bar{\boldsymbol{y}} = \boldsymbol{y}$. Such transformations are usually given as a composition of smaller augmentations including random crops, flips, color-jittering etc. In Fig. 1b we show a set of different augmentations of the same underlying image $\boldsymbol{x}$. Notice how these transformations indeed leave the associated label invariant. We denote by $\mathcal{T}$ the set of all possible augmentations. Data augmentation is usually applied in an online fashion, i.e. at every step of gradient descent, we uniformly sample a fresh transformation $T \sim \mathcal{U}(\mathcal{T})$ and propagate it through the network. We highlight that data augmentation is a standard technique necessary for state-of-the-art performance for a variety of vision tasks. Indeed, the top five leaders on *ImageNet*[1] (Yu et al., 2022; Dai et al., 2021; Zhai et al., 2021; Pham et al., 2021; Liu et al., 2021) all rely on some form of data augmentation in their training pipeline. If one hence wants to study the memorization potential of neural networks in practical settings, data augmentation needs to be considered. We notice that the results of Zhang et al. (2017) and subsequent studies on the properties of memorization under random labels (Arpit et al., 2017; Maennel et al., 2020) were obtained without the use of data augmentation, leaving the memorization picture thus incomplete.

[1] https://paperswithcode.com/sota/image-classification-on-imagenet

DATASET	MODEL	RANDOM	RANDOM + DA	CLEAN	CLEAN + DA	INIT
CIFAR10	*ResNet18*	12.4	76.2	83.6	91.3	40.6
	VGG11	15.0	69.1	83.0	89.0	44.3
CIFAR100	*ResNet18*	5.0	42.7	50.5	70.2	16.6
	VGG11	6.0	39.2	51.2	59.0	18.9
TinyImageNet	*ResNet18*	2.4	33.4	38.3	46.6	4.6
	VGG11	1.2	21.8	34.6	41.7	5.4

Table 2: K-NN probing accuracies (in percentage) of the embeddings for various datasets under different settings. DA refers to training under data augmentation. INIT refers to the performance at initialization. Except for INIT, all models reach perfect (unaugmented) training accuracy.

4 BENIGN MEMORIZATION

In this section, we present the curious phenomenon of benign memorization i.e. how neural networks manage to completely fit random labels under data augmentation, while at the same time learning predictive features for downstream tasks. Let us first formally introduce the terms *benign* and *malign* memorization, which are central to the results of this work. In the following, $\mathcal{S} := \{(\boldsymbol{x}_i, \boldsymbol{y}_i)\}_{i=1}^n$ denotes the original *clean* dataset and $\tilde{\mathcal{S}} = \{(\boldsymbol{x}_i, \tilde{\boldsymbol{y}}_i)\}_{i=1}^n$ its randomly labeled version.

Definition 4.1 *We call an encoder-projector pair $(h_{\boldsymbol{\phi}_*}, g_{\boldsymbol{\psi}_*})$ a **memorization** of $\tilde{\mathcal{S}}$, if f_* perfectly fits $\tilde{\mathcal{S}}$. Moreover, we call $(h_{\boldsymbol{\phi}_*}, g_{\boldsymbol{\psi}_*})$ a **malign** memorization if additionally, probing of $h_{\boldsymbol{\phi}_*}$ on $\mathcal{S}$ does not improve over probing at initialization. On the contrary, we call $(h_{\boldsymbol{\phi}_*}, g_{\boldsymbol{\psi}_*})$ a **benign** memorization of $\tilde{\mathcal{S}}$ if probing of $h_{\boldsymbol{\phi}_*}$ on $\mathcal{S}$ outperforms probing at initialization.*

As highlighted in Sec. 3 and shown in Table 2, memorizing solutions found with stochastic gradient descent without data augmentation on standard vision benchmarks are of malign nature. This is very intuitive, as randomizing the targets destroys any signal present in the dataset and thus generalization seems impossible. We show now how including data augmentation in the training pipeline completely reverses this observation.

Training details. In all subsequent experiments involving data augmentations, we use the standard transformations employed in self-supervised learning frameworks such as Chen et al. (2020c); Grill et al. (2020); Chen & He (2021). These consist of a composition of random crops, color-jittering, random greyscaling and random horizontal flips, leading to a diverse set of transformations. Moreover, we rely on mixup augmentations Zhang et al. (2018), where two images $\boldsymbol{x}_1$, $\boldsymbol{x}_2$ are combined into a linear interpolation, according to some weighting $\alpha \in [0, 1]$, i.e. $\bar{\boldsymbol{x}} := \alpha \boldsymbol{x}_1 + (1 - \alpha)\boldsymbol{x}_2$. The corresponding label $\bar{\boldsymbol{y}}$ is accordingly subject to the same linear combination, i.e. $\bar{\boldsymbol{y}} = \alpha \boldsymbol{y}_1 + (1 - \alpha)\boldsymbol{y}_2$ where labels are represented as their one-hot encodings. We use the standard vision datasets *CIFAR10* and *CIFAR100* (Krizhevsky & Hinton, 2009), as well as *TinyImageNet* (Le & Yang, 2015). For more details, we refer the reader to Appendix D.

Benign Memorization. We display the results of training under data augmentation in Table 2. We observe that, surprisingly, nearest-neighbour probing of the learnt embeddings leads to clearly non-trivial performance, strongly improving over the models trained under random labels without data augmentation. Moreover, we strongly outperform probing at initialization, showing that indeed rich feature learning is happening. As a consequence, data augmentation does not simply prevent malign memorization by preserving the signal at initialization but actually leads to learning from the data. On the other hand, it holds that the projector achieves perfect training accuracy on the random labels and the network thus indeed memorizes the training data perfectly. Under data augmentation, deep models hence exhibit benign memorization. In Appendix B, Fig. 9, we further underline the utility of the learnt features by evaluating their performance under transfer learning. We remark that this is, to the best of our knowledge, the first work showing that learning under random labels can lead to strong downstream performance, highlighting that memorization and generalization are not necessarily at odds. We notice that the training time under randomized targets together with data

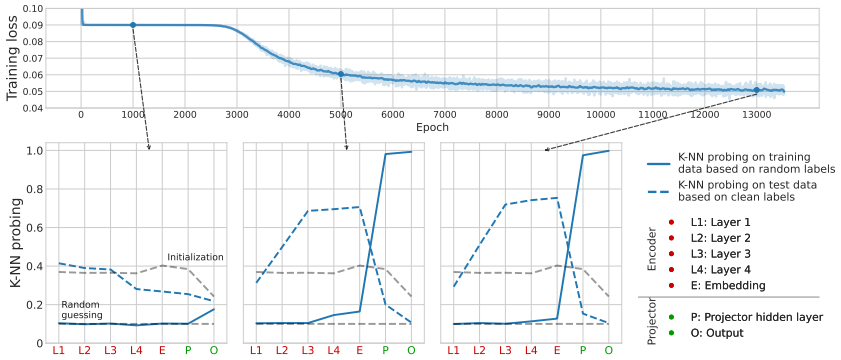

Figure 3: K-NN probing of a *ResNet18* on *CIFAR10*, based on (flattened) representation of different layers. Dashed blue lines indicate K-NN accuracies fitted on the clean training data and evaluated w.r.t. clean test data. Solid lines indicate K-NN training accuracies based on the random labels. Notice the sharp phase transition when reaching the projector layers"P" and "O", i.e. the projector reaches strong performance on the noisy labels (dashed) but randomly guesses on the clean data (solid). The opposite happens for the embedding layer, reaching 76% K-NN accuracy.

augmentation increases significantly, both compared to training under clean labels as well as fitting random labels without augmentations. In Fig. 3 we show the evolution of both the training loss as well as nearest-neighbour probing test accuracy as a function of the number of epochs. Observe that for as long as 3000 epochs, neither training loss nor probing accuracy show any progress but then suddenly start to rapidly improve.

We stress that our goal is not to compete with standard training under clean labels, it can be seen in Table 2 that there is a large gap between the two methods. Instead we rather aim for a deeper understanding of how deep networks generalize. We show that generalization, contrary to prior beliefs, remains possible even in the most adversarial setting of complete label noise.

Signal-Noise Separation. We now further inspect models trained under random labels and data augmentation, with an emphasis on how the noise stemming from the random labeling affects different parts of the network. To gain insights into this, we perform nearest-neighbour probing of different layers in the network, with the twist that we fit the K-NN classifier both with respect to the clean training labels, as well as with respect to the random labels. This way we can assess how much a given feature has adapted to the particular structure (clean vs. random). We visualize the results of such a clean and noisy probing strategy in Fig. 3 at different stages of training. Surprisingly, we can see a striking separation between feature learning and memorization within the architecture; noisy probing only starts to improve over random guessing once we reach the projector, whereas the encoder remains largely unaffected. On the other hand, clean probing outperforms probing at initialization throughout the entire embedding stage but sharply decays once we get to the projector. While previous works have identified that the very first layers provide non-trivial performance even without data augmentation, including it strengthens this effect significantly. We give an interpretation of this finding in Sec. 5.2. We further investigate the role of the projector in Appendix B, Fig. 7, finding that higher widths lead to better performance in general.

5 The Role of Augmentations

The empirical evidence in the previous section highlights the crucial role of data augmentation for benign memorization. In this section, we aim to gain insights into the phenomenon by investigating more closely what properties of data augmentation are essential for benign memorization and how "ideal" augmentations might strongly differ when learning with clean or random labels.

Label Preservation. The first important characteristic of augmentations is their label-preserving nature, i.e. by augmenting an image $(\boldsymbol{x}, \boldsymbol{y})$ twice to produce $(T_1(\boldsymbol{x}), \boldsymbol{y}), (T_2(\boldsymbol{x}), \boldsymbol{y})$, we have effectively added information, as indeed $T_1(\boldsymbol{x})$ and $T_2(\boldsymbol{x})$ share the same label. Unfortunately, this reasoning is flawed in the setting of random labels, or at the least only forms part of a larger picture, as we show in the following *thought experiment*. Consider two "original" samples $(\boldsymbol{x}_1, \tilde{\boldsymbol{y}})$ and

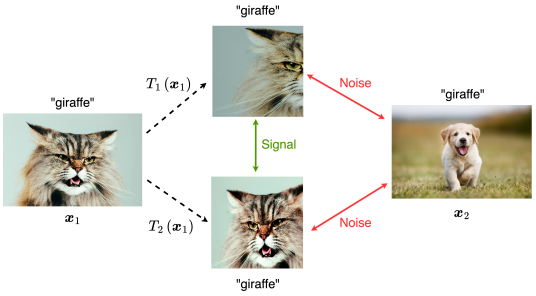

Figure 4: Illustration of the thought experiment in Sec. 5. The true cat $\boldsymbol{x}_1$ labeled as "giraffe" is augmented, leading to a positive signal between the augmentations but to more noise due to $\boldsymbol{x}_2$, that has as true label "dog".

Dataset Size	1000	50000
Random	11.41	12.41
Random + i.i.d. DA	12.41	-
Clean	36.75	83.66
Clean + i.i.d. DA	82.73	-

Table 3: K-NN probing accuracies of the embeddings of a *ResNet18* for *CIFAR10* with and without i.i.d. augmentations under clean and random labels. 50000 refers to full *CIFAR10* for reference.

$(\boldsymbol{x}_2, \tilde{\boldsymbol{y}})$ which happen to share the same random label $\tilde{\boldsymbol{y}}$ but in truth have distinct labels $\boldsymbol{y}_1 \neq \boldsymbol{y}_2$. In this case, forming augmentations $(T_1(\boldsymbol{x}_1), \tilde{\boldsymbol{y}})$ and $(T_2(\boldsymbol{x}_1), \tilde{\boldsymbol{y}})$ might lead to some correct signal as $T_1(\boldsymbol{x}_1)$ and $T_2(\boldsymbol{x}_1)$ share the same, true label, but at the same time leads to more distortion as $\boldsymbol{x}_2$ has the same, random label, reinforcing the wrong correlation even more. As a consequence, separating noise from signal remains equally challenging as before. We illustrate the argument in Fig. 4. To check this hypothesis, we consider the extreme case where augmentations $T \in \mathcal{T}$ produce a new, i.i.d. sample $T(\boldsymbol{x})$ that shares the same, true label with $\boldsymbol{x}$. In a sense, this is the ideal augmentation and leads to the highest information gain. We implement such augmentations by only using a subset of the training data while using the remainder to assign to each training point B potential, independent examples with the same, true label. We choose the subset size as $s = 1000$ and the number of augmentations as $B = 50$ for *CIFAR10* and train the same models as in Sec. 4, both under random and clean labels. We display the results in Table 4. Notice that for clean label training, such augmentations increase the training set size from 1000 to $1000 \times 50 = 50000$, thus leading to almost identical performance as training on the full dataset. Counter-intuitively, but for the reasons outlined above, training under random labels severely suffers under such ideal, independent augmentations and leads to malign memorization. In fact, this experiment is equivalent to fitting random labels without augmentations on the full training set where malign memorization occurs, as seen in Sec. 4.

This thought experiment demonstrates that under random labels, augmentations seem to play a very distinct role compared to the clean setting and label preservation in itself is not enough to guarantee benign memorization. This raises the following question:

What other properties of augmentations, besides label preservation, cause benign memorization?

We hypothesize that the origins of the phenomenon lie at the interplay between the highly correlated nature of augmentations and the inflated effective sample size that exceeds the model capacity (Sec 5.1), forcing the model to learn meaningful features (Sec 5.2).

5.1 Going Beyond the Model Capacity

We now study the phenomenon of benign memorization from the view point of capacity of a model class. Intuitively speaking, the capacity of a model captures how many distinct datapoints we can fit, even if the corresponding targets are completely randomized. If a model has enough capacity, it can potentially memorize all the patterns in the dataset. As seen in Zhang et al. (2017), deep models used in practice in conjunction with standard datasets, operate below the capacity threshold but nevertheless, they do not "abuse" their power and fit clean data in a meaningful way. On the other hand, by using data augmentation we inflate the number of samples and consequently operate above the capacity level. As a result, a model needs to *efficiently* encode augmentations (pure memorization is not possible) and hence meaningful features need to be learnt. We start by mathematically introducing the concept of capacity of a model class trained with Gradient Descent (GD). We remark that similar definitions have been explored in prior work (Arpit et al., 2017).

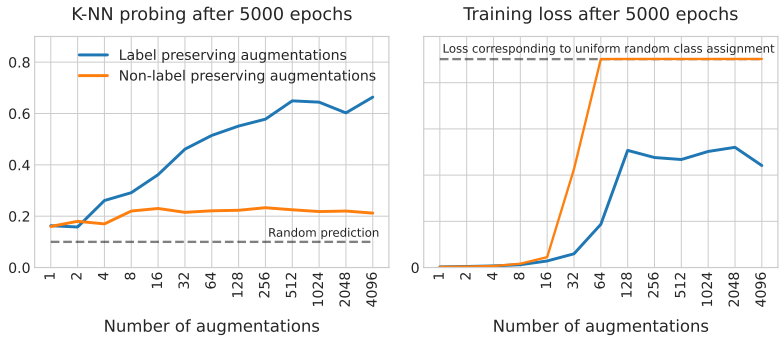

Figure 5: Illustration of nearest-neighbour probing accuracy (left) and training loss (right) of a *ResNet18* on *CIFAR10* with increasing number of augmentations. We consider both label-preserving (blue) and completely random labeling of augmentations (red).

Definition 5.1 *Consider $\boldsymbol{x}_1, \ldots, \boldsymbol{x}_n$ for $n \in \mathbb{N}$ in general position and a fixed number of classes C. Given a labeling $\tilde{\mathcal{S}} = \{(\boldsymbol{x}_i, \tilde{\boldsymbol{y}}_i)\}_{i=1}^n$, let $\mathcal{A}_t(\tilde{\mathcal{S}}) \subset \Theta$ denote the set of solutions reachable by GD with a computational budget t. We define the capacity $\mathcal{C}_t$ of the model class $\{f_{\boldsymbol{\theta}} : \boldsymbol{\theta} \in \Theta\}$ as*

$$\mathcal{C}_t := sup\{n \in \mathbb{N} | \, \forall \tilde{\mathcal{S}} \; \exists \boldsymbol{\theta} \in \mathcal{A}_t(\tilde{\mathcal{S}}) \; s.t. \; f_{\boldsymbol{\theta}} \; memorizes \; \tilde{\mathcal{S}}\}.$$

While similar to standard measures such as the VC-dimension (Vapnik & Chervonenkis, 1971), the capacity defined here depends on the learning algorithm (including the computational budget t), and is thus always smaller than the corresponding VC-dimension. As seen in Sec. 3, standard datasets such as *CIFAR10* have size n below the capacity $\mathcal{C}_t$ of modern networks such as *ResNets*. When using data augmentation however, we now show that the resulting dataset exceeds the capacity.

Inflated Sample Size. Consider a set of augmentations $\mathcal{T}$ and assume that it has a finite size, $B := |\mathcal{T}| < \infty$. Augmenting thus leads to a larger effective dataset $\mathcal{S}_{\text{aug}}$ of size Bn. We can now study whether the capacity of standard networks trained by GD for a fixed number of epochs exceeds such an augmented dataset by varying B and randomly labeling each sample. We pre-compute a fixed set of B random augmentations for each sample for varying B and attempt to memorize a random labeling, where labels of augmentations are **not** preserved. We use the same setup as in Sec. 4 and augment *CIFAR10* using the standard augmentations in the way described above. We display the results in Fig. 5. We see that indeed, overfitting the random labels becomes more difficult as we increase B and actually infeasible for a fixed number of gradient steps $t = 5000 \times 196$ (fixed batch size on *CIFAR10*). Moreover, totice that in the standard setting of online augmentations, this observation becomes even more drastic as effectively $B \to \infty$ if typical, continuous augmentations such as color jittering are included in the pipeline. We hypothesize that malign memorization under such an augmentation strategy thus becomes infeasible.

Learn if you must. We now investigate the influence of capacity on the resulting probing accuracy, in the case where augmentations are label-preserving and thus offer valuable signal. We thus consider the same setup as in the previous paragraph for varying number of augmentations B while assigning the same label to augmentations of the same image. We show the results in Fig. 5 on the left. We observe that as the number of augmentations B increases, probing accuracy improves and eventually surpasses probing at initialization. We hypothesize that as we approach and eventually surpass capacity, the model is increasingly forced to leverage the signal in augmentations and thus learns more and more relevant features. As we increase B, we saturate the information gain provided by the augmentations, the signal becomes redundant and performance starts to plateau.

5.2 What can you Learn from Augmentations?

While we have seen that the model is forced to leverage the signal in augmentations, it remains unclear why this leads to high-quality embeddings. We now show how augmentations encourage features to become invariant, a property that has been identified in SSL to be strongly predictive.

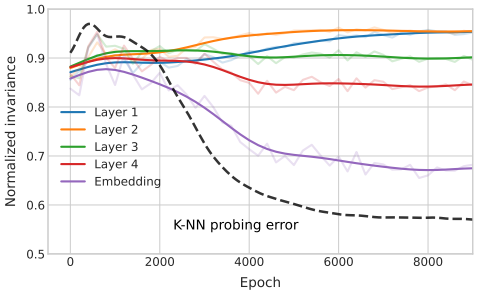

Method	Normalized invariance
Initialization	0.867
Clean	0.912
Clean + DA	0.691
Random	0.989
Random + DA	0.680

Figure 6: Normalized invariance of a *ResNet18* on *CIFAR10*, as a function of epochs, lower value means more invariant. The dashed line represents K-NN probing error (scaled for comparability).

Normalized Invariance. To measure the invariance of a model $f_{\boldsymbol{\theta}}$, we introduce the following quantity:

$$I(\boldsymbol{x}; f_{\boldsymbol{\theta}}, \mathcal{T}) := \frac{\mathbb{E}_{T_1,T_2\sim\mathcal{U}(\mathcal{T})}\|f_{\boldsymbol{\theta}}(T_1(\boldsymbol{x})) - f_{\boldsymbol{\theta}}(T_2(\boldsymbol{x}))\|}{\mathbb{E}_{\boldsymbol{x}'\neq\boldsymbol{x}}\|f_{\boldsymbol{\theta}}(\boldsymbol{x}) - f_{\boldsymbol{\theta}}(\boldsymbol{x}')\|}. \tag{2}$$

Intuitively, $I(\boldsymbol{x}; f_{\boldsymbol{\theta}}, \mathcal{T})$ captures the features' similarity of augmentations of the same datapoint $\boldsymbol{x}$ compared to the representations of different datapoints $\boldsymbol{x}' \neq \boldsymbol{x}$. Model's invariance implies $I(\boldsymbol{x}; f_{\boldsymbol{\theta}}, \mathcal{T}) = 0$, hence different augmentations are mapped to the same datapoint, while the model is still able to meaningfully distinguish between the representations of different datapoints (i.e. $\mathbb{E}_{\boldsymbol{x}'\neq\boldsymbol{x}}\|f_{\boldsymbol{\theta}}(\boldsymbol{x}) - f_{\boldsymbol{\theta}}(\boldsymbol{x}')\| \neq 0$). In Fig. 6, we show how $I(\boldsymbol{x}; f, \mathcal{T})$ correlates with probing performance and indeed decreases over time. Due to its better implicit bias (*ResNet* vs MLP), invariance is largely learnt in the encoder, leading to the striking signal-noise separation identified in Sec. 4. These results suggest that when the model has insufficient capacity to memorize the (augmented) samples, it learns to be more invariant with respect to the label-preserving augmentations. Consequently, this mechanism reduces the "effective sample size" and allows the model to fit the data in a *benign* (i.e. augmentation-invariant) way. But why do invariant features imply a better clustering in embedding space as evidenced by a high K-NN accuracy? This is a heavily researched topic with several plausible theories in the area of self-supervised learning (SSL) (Saunshi et al., 2022; Arora et al., 2019b; Wen & Li, 2021). In Appendix A, we derive a more formal connection between SSL loss and training with random labels. Others have looked at the improved sample complexity caused by incorporating invariances into the model (Bietti et al., 2021; Xiao & Pennington, 2022).

6 Discussion and Conclusion

In this work we have identified the surprising phenomenon of benign memorization, demonstrating that generalization and memorization are not necessarily at odds. We put forward an interpretation through the lens of model capacity, where the inflation in sample size forces the model to exploit the correlation structure by learning the invariance with respect to the augmentations. Furthermore, we have shown that invariance learning happens largely in the encoder, while the projector performs the noisy memorization task.

Our findings underline the complicated and mysterious inner workings of neural networks, showing that generalization can be found where we least expect it. To describe benign memorization, a complete generalization theory needs to capture the strong implicit bias built into deep models, which enables a clean separation of noise and signal. Secondly, such a theory needs to incorporate feature learning, as benign memorization only emerges in the encoder. Both those goals remain very challenging. In particular, we speculate that the line of work based on the *neural tangent kernel* (Jacot et al., 2018) which connects SGD-optimized neural networks in the infinite width regime and the realm of kernels cannot explain benign memorization. In fact, in this regime the weights do not move from initialization, thus preventing feature learning. On the other hand, approaches that aim at computing perturbative finite width corrections to these kernels (Hanin & Nica, 2019; Zavatone-Veth et al., 2021) might be a promising approach to explain the phenomenon of benign memorization, as they incorporate feature learning. We leave exploring benign memorization in such a mathematical framework as future work.

7 REPRODUCIBILITY STATEMENT

We refer the reader to Appendix D for a complete description of the training protocol.

REFERENCES

Guillaume Alain and Yoshua Bengio. Understanding intermediate layers using linear classifier probes. *International Conference on Learning Representations (ICLR)*, abs/1610.01644, 2017.

Sanjeev Arora, Rong Ge, Behnam Neyshabur, and Yi Zhang. Stronger generalization bounds for deep nets via a compression approach. *Proceedings of the 35th International Conference on Machine Learning (ICML)*, 2018.

Sanjeev Arora, Simon S. Du, Wei Hu, Zhiyuan Li, and Ruosong Wang. Fine-grained analysis of optimization and generalization for overparameterized two-layer neural networks. *Proceedings of the 36th International Conference on Machine Learning (ICML*, 2019a.

Sanjeev Arora, Hrishikesh Khandeparkar, Mikhail Khodak, Orestis Plevrakis, and Nikunj Saunshi. A theoretical analysis of contrastive unsupervised representation learning. *arXiv preprint arXiv:1902.09229*, 2019b.

Devansh Arpit, Stanisław Jastrzebski, Nicolas Ballas, David Krueger, Emmanuel Bengio, Maxinder S Kanwal, Tegan Maharaj, Asja Fischer, Aaron Courville, Yoshua Bengio, et al. A closer look at memorization in deep networks. In *International conference on machine learning*, pp. 233–242. PMLR, 2017.

Adrien Bardes, Jean Ponce, and Yann LeCun. VICReg: Variance-invariance-covariance regularization for self-supervised learning. In *International Conference on Learning Representations (ICLR)*, 2022.

Peter Bartlett, Dylan J. Foster, and Matus Telgarsky. Spectrally-normalized margin bounds for neural networks. *31st Conference on Neural Information Processing Systems (Neurips)*, 2017.

Peter L. Bartlett, Nick Harvey, Chris Liaw, and Abbas Mehrabian. Nearly-tight vc-dimension and pseudodimension bounds for piecewise linear neural networks. *Journal of Machine Learning Research 20*, pp. 1–17, 2019.

Peter L. Bartlett, Philip M. Long, Gá bor Lugosi, and Alexander Tsigler. Benign overfitting in linear regression. *Proceedings of the National Academy of Sciences*, 117(48):30063–30070, apr 2020. doi: 10.1073/pnas.1907378117.

Alberto Bietti, Luca Venturi, and Joan Bruna. On the sample complexity of learning under geometric stability. *Advances in Neural Information Processing Systems*, 34:18673–18684, 2021.

Mathilde Caron, Hugo Touvron, Ishan Misra, Herv'e J'egou, Julien Mairal, Piotr Bojanowski, and Armand Joulin. Emerging properties in self-supervised vision transformers. *2021 IEEE/CVF International Conference on Computer Vision (ICCV)*, pp. 9630–9640, 2021.

Mark Chen, Alec Radford, Jeff Wu, Heewoo Jun, Prafulla Dhariwal, David Luan, and Ilya Sutskever. Generative pretraining from pixels. In *Proceedings of the 37th International Conference on Machine Learning (ICML)*, 2020a.

Shuxiao Chen, Edgar Dobriban, and Jane Lee. A group-theoretic framework for data augmentation. In H. Larochelle, M. Ranzato, R. Hadsell, M. F. Balcan, and H. Lin (eds.), *Advances in Neural Information Processing Systems*, volume 33, pp. 21321–21333. Curran Associates, Inc., 2020b.

Ting Chen, Simon Kornblith, Mohammad Norouzi, and Geoffrey Hinton. A simple framework for contrastive learning of visual representations. In Hal Daumé III and Aarti Singh (eds.), *Proceedings of the 37th International Conference on Machine Learning*, volume 119 of *Proceedings of Machine Learning Research*, pp. 1597–1607. PMLR, 13–18 Jul 2020c.

Xinlei Chen and Kaiming He. Exploring simple siamese representation learning. In *Proceedings of the IEEE/CVF Conference on Computer Vision and Pattern Recognition*, pp. 15750–15758, 2021.

Adam Coates, Andrew Ng, and Honglak Lee. An analysis of single-layer networks in unsupervised feature learning. In Geoffrey Gordon, David Dunson, and Miroslav Dudík (eds.), *Proceedings of the Fourteenth International Conference on Artificial Intelligence and Statistics (AISTATS)*, volume 15 of *Proceedings of Machine Learning Research*, pp. 215–223, Fort Lauderdale, FL, USA, 11–13 Apr 2011. PMLR.

Gilad Cohen, Guillermo Sapiro, and Raja Giryes. Dnn or k-nn: That is the generalize vs. memorize question. *ArXiv*, abs/1805.06822, 2018.

Ekin D Cubuk, Barret Zoph, Jonathon Shlens, and Quoc V Le. Randaugment: Practical automated data augmentation with a reduced search space. In *Proceedings of the IEEE/CVF conference on computer vision and pattern recognition workshops*, pp. 702–703, 2020.

Zihang Dai, Hanxiao Liu, Quoc V Le, and Mingxing Tan. Coatnet: Marrying convolution and attention for all data sizes. In A. Beygelzimer, Y. Dauphin, P. Liang, and J. Wortman Vaughan (eds.), *Advances in Neural Information Processing Systems*, 2021.

Tri Dao, Albert Gu, Alexander Ratner, Virginia Smith, Chris De Sa, and Christopher Re. A kernel theory of modern data augmentation. In Kamalika Chaudhuri and Ruslan Salakhutdinov (eds.), *Proceedings of the 36th International Conference on Machine Learning*, volume 97 of *Proceedings of Machine Learning Research*, pp. 1528–1537. PMLR, 09–15 Jun 2019.

Jia Deng, Wei Dong, Richard Socher, Li-Jia Li, Kai Li, and Li Fei-Fei. Imagenet: A large-scale hierarchical image database. In *2009 IEEE Conference on Computer Vision and Pattern Recognition*, pp. 248–255, 2009. doi: 10.1109/CVPR.2009.5206848.

Jacob Devlin, Ming-Wei Chang, Kenton Lee, and Kristina Toutanova. Bert: Pre-training of deep bidirectional transformers for language understanding. *Proceedings of NAACL-HLT*, 2019.

Alexey Dosovitskiy, Jost Tobias Springenberg, Martin Riedmiller, and Thomas Brox. Discriminative unsupervised feature learning with convolutional neural networks. *Advances in neural information processing systems*, 27, 2014.

Gintare Karolina Dziugaite and Daniel M. Roy. Computing nonvacuous generalization bounds for deep (stochastic) neural networks with many more parameters than training data. *Proceedings of the Thirty-Third Conference on Uncertainty in Artificial Intelligence*, 2017.

Vitaly Feldman and Chiyuan Zhang. What neural networks memorize and why: Discovering the long tail via influence estimation. *Advances in Neural Information Processing Systems*, 33:2881–2891, 2020.

Spencer Frei, Niladri S Chatterji, and Peter Bartlett. Benign overfitting without linearity: Neural network classifiers trained by gradient descent for noisy linear data. In Po-Ling Loh and Maxim Raginsky (eds.), *Proceedings of Thirty Fifth Conference on Learning Theory*, volume 178 of *Proceedings of Machine Learning Research*, pp. 2668–2703. PMLR, 02–05 Jul 2022.

Jean-Bastien Grill, Florian Strub, Florent Altché, Corentin Tallec, Pierre Richemond, Elena Buchatskaya, Carl Doersch, Bernardo Avila Pires, Zhaohan Guo, Mohammad Gheshlaghi Azar, Bilal Piot, koray kavukcuoglu, Remi Munos, and Michal Valko. Bootstrap your own latent - a new approach to self-supervised learning. In H. Larochelle, M. Ranzato, R. Hadsell, M.F. Balcan, and H. Lin (eds.), *Advances in Neural Information Processing Systems*, volume 33, pp. 21271–21284. Curran Associates, Inc., 2020.

Boris Hanin and Mihai Nica. Finite depth and width corrections to the neural tangent kernel. *arXiv preprint arXiv:1909.05989*, 2019.

Boris Hanin and Yi Sun. How data augmentation affects optimization for linear regression. In A. Beygelzimer, Y. Dauphin, P. Liang, and J. Wortman Vaughan (eds.), *Advances in Neural Information Processing Systems*, 2021.

Kaiming He, Xiangyu Zhang, Shaoqing Ren, and Jian Sun. Deep residual learning for image recognition. *IEEE Conference on Computer Vision and Pattern Recognition (CVPR)*, 2016.

Tianyu Hua, Wenxiao Wang, Zihui Xue, Sucheng Ren, Yue Wang, and Hang Zhao. On feature decorrelation in self-supervised learning. In *Proceedings of the IEEE/CVF International Conference on Computer Vision*, pp. 9598–9608, 2021a.

Tianyu Hua, Wenxiao Wang, Zihui Xue, Yue Wang, Sucheng Ren, and Hang Zhao. On feature decorrelation in self-supervised learning. *2021 IEEE/CVF International Conference on Computer Vision (ICCV)*, pp. 9578–9588, 2021b.

Arthur Jacot, Franck Gabriel, and Clément Hongler. Neural tangent kernel: Convergence and generalization in neural networks. *Advances in neural information processing systems*, 31, 2018.

Thomas N. Kipf and Max Welling. Semi-supervised classification with graph convolutional networks. *Proceedings of the 5th International Conference on Learning Representations*, 2017.

Alex Krizhevsky and Geoffrey Hinton. Learning multiple layers of features from tiny images. Technical Report 0, University of Toronto, Toronto, Ontario, 2009.

Ya Le and Xuan S. Yang. Tiny imagenet visual recognition challenge. 2015.

Ze Liu, Han Hu, Yutong Lin, Zhuliang Yao, Zhenda Xie, Yixuan Wei, Jia Ning, Yue Cao, Zheng Zhang, Li Dong, Furu Wei, and Baining Guo. Swin transformer v2: Scaling up capacity and resolution, 2021.

Siyuan Ma, Raef Bassily, and Mikhail Belkin. The power of interpolation: Understanding the effectiveness of SGD in modern over-parametrized learning. In Jennifer Dy and Andreas Krause (eds.), *Proceedings of the 35th International Conference on Machine Learning*, volume 80 of *Proceedings of Machine Learning Research*, pp. 3325–3334. PMLR, 10–15 Jul 2018.

Hartmut Maennel, Ibrahim M Alabdulmohsin, Ilya O Tolstikhin, Robert Baldock, Olivier Bousquet, Sylvain Gelly, and Daniel Keysers. What do neural networks learn when trained with random labels? *Advances in Neural Information Processing Systems*, 33:19693–19704, 2020.

Behnam Neyshabur, Ryota Tomioka, and Nathan Srebro. Norm-based capacity control in neural networks. *Proceedings of The 28th Conference on Learning Theory (PMLR)*, 2015.

Behnam Neyshabur, Srinadh Bhojanapalli, and Nathan Srebro. A pac-bayesian approach to spectrally-normalized margin bounds for neural networks. *International Conference on Learning Representations (ICLR)*, 2018.

Kento Nishi, Yi Ding, Alex Rich, and Tobias Höllerer. Augmentation strategies for learning with noisy labels. *2021 IEEE/CVF Conference on Computer Vision and Pattern Recognition (CVPR)*, pp. 8018–8027, 2021.

Giorgio Patrini, Alessandro Rozza, Aditya Krishna Menon, Richard Nock, and Lizhen Qu. Making deep neural networks robust to label noise: A loss correction approach. *2017 IEEE Conference on Computer Vision and Pattern Recognition (CVPR)*, pp. 2233–2241, 2017.

Hieu Pham, Zihang Dai, Qizhe Xie, Minh-Thang Luong, and Quoc V. Le. Meta pseudo labels. In *IEEE Conference on Computer Vision and Pattern Recognition*, 2021.

Vinaychandran Pondenkandath, Michele Alberti, Sammer Puran, Rolf Ingold, and Marcus Liwicki. Leveraging random label memorization for unsupervised pre-training. *Workshop of Integration of Deep Learning Theories at Conference on Neural Information Processing Systems (NIPS)*, abs/1811.01640, 2018.

David Rolnick, Andreas Veit, Serge Belongie, and Nir Shavit. Deep learning is robust to massive label noise. *arXiv preprint arXiv:1705.10694*, 2017.

Amartya Sanyal, Puneet K. Dokania, Varun Kanade, and Philip Torr. How benign is benign overfitting? In *International Conference on Learning Representations*, 2021.

Nikunj Saunshi, Jordan Ash, Surbhi Goel, Dipendra Misra, Cyril Zhang, Sanjeev Arora, Sham Kakade, and Akshay Krishnamurthy. Understanding contrastive learning requires incorporating inductive biases. *Proceedings of the 39th International Conference on Machine Learning, (ICML)*, 2022.

Karen Simonyan and Andrew Zisserman. Very deep convolutional networks for large-scale image recognition. *International Conference on Learning Representations (ICLR)*, 2014.

Hwanjun Song, Minseok Kim, Dongmin Park, Yooju Shin, and Jae-Gil Lee. Learning from noisy labels with deep neural networks: A survey, 2020.

Nitish Srivastava, Geoffrey Hinton, Alex Krizhevsky, Ilya Sutskever, and Ruslan Salakhutdinov. Dropout: A simple way to prevent neural networks from overfitting. *Journal of Machine Learning Research*, 15(56):1929–1958, 2014.

V. N. Vapnik and A. Ya. Chervonenkis. On the uniform convergence of relative frequencies of events to their probabilities. *Theory of Probability and its Applications*, 16(2):264–280, 1971. doi: 10.1137/1116025.

Zixin Wen and Yuanzhi Li. Toward understanding the feature learning process of self-supervised contrastive learning. In *International Conference on Machine Learning*, pp. 11112–11122. PMLR, 2021.

Sen Wu, Hongyang R. Zhang, Gregory Valiant, and Christopher Ré. On the generalization effects of linear transformations in data augmentation. In *Proceedings of the 37th International Conference on Machine Learning (ICML)*, 2020.

Lechao Xiao and Jeffrey Pennington. Synergy and symmetry in deep learning: Interactions between the data, model, and inference algorithm. *arXiv preprint arXiv:2207.04612*, 2022.

Jiahui Yu, Zirui Wang, Vijay Vasudevan, Legg Yeung, Mojtaba Seyedhosseini, and Yonghui Wu. Coca: Contrastive captioners are image-text foundation models. *Transactions on Machine Learning Research*, 2022.

Jacob Zavatone-Veth, Abdulkadir Canatar, Ben Ruben, and Cengiz Pehlevan. Asymptotics of representation learning in finite bayesian neural networks. *Advances in neural information processing systems*, 34:24765–24777, 2021.

Jure Zbontar, Li Jing, Ishan Misra, Yann LeCun, and Stéphane Deny. Barlow twins: Self-supervised learning via redundancy reduction. In *Proceedings of the 38th International Conference on Machine Learning (ICML*.

Xiaohua Zhai, Alexander Kolesnikov, Neil Houlsby, and Lucas Beyer. Scaling vision transformers, 2021.

Chiyuan Zhang, Samy Bengio, Moritz Hardt, Benjamin Recht, and Oriol Vinyals. Understanding deep learning requires rethinking generalization. *International Conference on Learning Representations (ICLR)*, 2017.

Hongyi Zhang, Moustapha Cisse, Yann N. Dauphin, and David Lopez-Paz. mixup: Beyond empirical risk minimization. In *International Conference on Learning Representations*, 2018.

Xuanyang Zhang, Pengfei Hou, X. Zhang, and Jian Sun. Neural architecture search with random labels. *2021 IEEE/CVF Conference on Computer Vision and Pattern Recognition (CVPR)*, pp. 10902–10911, 2021.

A CONNECTION TO SELF SUPERVISED LEARNING

In this section, we investigate the connection between non-contrastive SSL (Hua et al., 2021b; Grill et al., 2020; Chen & He, 2021) and training with random labels on the mean squared error (MSE) loss. We start with the following result:

Lemma A.1 *Fix $B \in \mathbb{N}$ vectors $\boldsymbol{x}_1, \dots, \boldsymbol{x}_B \in \mathbb{R}^d$ and $\boldsymbol{a} \in \mathbb{R}^d$. Then it holds that*

$$\frac{1}{B}\sum_{i=1}^{B} \|\boldsymbol{x}_i - \boldsymbol{a}\|^2 = \frac{1}{2B^2}\sum_{i,j=1}^{B} \|\boldsymbol{x}_i - \boldsymbol{x}_j\|^2 + \|\boldsymbol{a} - \frac{1}{B}\sum_{i=1}^{B} \boldsymbol{x}_i\|^2$$

Proof: We simply expand the first term on the right-hand-side:

$$\begin{aligned}
\frac{1}{2B^2}\sum_{i,j=1}^{B} \|\boldsymbol{x}_i - \boldsymbol{x}_j\|^2 &= \frac{1}{2B^2}\sum_{i,j=1}^{B} \|\boldsymbol{x}_i - \boldsymbol{a} + \boldsymbol{a} - \boldsymbol{x}_j\|^2 \\
&= \frac{1}{2B^2}\left(\sum_{i,j=1}^{B} \|\boldsymbol{x}_i - \boldsymbol{a}\|^2 + \|\boldsymbol{x}_j - \boldsymbol{a}\|^2 - 2(\boldsymbol{x}_i - \boldsymbol{a})^T(\boldsymbol{x}_j - \boldsymbol{a})\right) \\
&= \frac{1}{B}\sum_{i}^{B} \|\boldsymbol{x}_i - \boldsymbol{a}\|^2 - \frac{1}{B^2}\sum_{i,j=1}^{B} (\boldsymbol{x}_i - \boldsymbol{a})^T(\boldsymbol{x}_j - \boldsymbol{a}) \\
&= \frac{1}{B}\sum_{i}^{B} \|\boldsymbol{x}_i - \boldsymbol{a}\|^2 - \|\boldsymbol{a}\|^2 - \frac{1}{B^2}\sum_{i,j=1}^{n} \boldsymbol{x}_i^T\boldsymbol{x}_j + \frac{2}{B}\sum_{i=1}^{n} \boldsymbol{a}^T\boldsymbol{x}_i
\end{aligned}$$

On the other hand, we have that

$$\|\boldsymbol{a} - \frac{1}{B}\sum_{i=1}^{B} \boldsymbol{x}_i\|^2 = \|\boldsymbol{a}\|^2 + \frac{1}{B^2}\sum_{i,j=1}^{n} \boldsymbol{x}_i^T\boldsymbol{x}_j - \frac{2}{B}\sum_{i=1}^{n} \boldsymbol{a}^T\boldsymbol{x}_i$$

Hence we see that

$$\frac{1}{2B^2}\sum_{i,j=1}^{B} \|\boldsymbol{x}_i - \boldsymbol{x}_j\|^2 = \frac{1}{B}\sum_{i}^{B} \|\boldsymbol{x}_i - \boldsymbol{a}\|^2 - \|\boldsymbol{a} - \frac{1}{B}\sum_{i=1}^{B} \boldsymbol{x}_i\|^2$$

and re-arranging terms concludes the proof.

We now apply this result in the case where the label plays the role of $\boldsymbol{a}$ and $\boldsymbol{x}_i$'s play the role of different augmentations. Let us thus consider B augmentations $T_1, \dots, T_B$ and $n \in \mathbb{N}$ samples $\boldsymbol{x}_1, \dots, \boldsymbol{x}_n \in \mathbb{R}^d$. Moreover we have some labels $\boldsymbol{y}_1, \dots, \boldsymbol{y}_n \in \mathbb{R}^K$ that could be completely random. Using the previous result we can write the (random) supervised loss (assuming mean-squared error) as follows:

Theorem A.2 *Denote the supervised loss under data augmentation as*

$$\hat{L}^{super}(\boldsymbol{\theta}) = \frac{1}{nB}\sum_{i=1}^{n}\sum_{a=1}^{B} \left\|f_{\boldsymbol{\theta}}(T_a(\boldsymbol{x}_i)) - \boldsymbol{y}_i\right\|^2$$

Then we can decompose it into the following two terms,

$$\hat{L}^{super}(\boldsymbol{\theta}) = \underbrace{\frac{1}{2nB^2}\sum_{i=1}^{n}\sum_{a,b=1}^{B} \left\|f_{\boldsymbol{\theta}}(T_a(\boldsymbol{x}_i)) - f_{\boldsymbol{\theta}}(T_b(\boldsymbol{x}_i))\right\|^2}_{=:\mathrm{Inv}(\boldsymbol{\theta})\geq 0} + \underbrace{\frac{1}{n}\sum_{i=1}^{n}\left\|\boldsymbol{y}_i - \frac{1}{B}\sum_{a=1}^{B} f_{\boldsymbol{\theta}}(T_a(\boldsymbol{x}_i))\right\|^2}_{=:\mathrm{Bias}(\boldsymbol{\theta})\geq 0}$$

Notice that in $\mathrm{Inv}(\boldsymbol{\theta})$, we group augmentations of the same input $\boldsymbol{x}_i$ together, measuring thus how invariant a given model $f_{\boldsymbol{\theta}}$ is w.r.t. to the augmentations. This is the positive signal illustrated in

the thought experiment in Fig. 4. Interestingly, minimizing $\text{Inv}(\boldsymbol{\theta})$ is a core ingredient for so-called non-contrastive self-supervised learning methods (Hua et al., 2021b; Grill et al., 2020; Chen & He, 2021).

The bias term on the other hand is influenced by the random labeling. To better understand the bias term, define $N_c := \{i \in \{1, \dots, n\} : \boldsymbol{y}_i = \boldsymbol{e}_c\}$, i.e. all samples that have label c. Furthermore, let $\bar{f}_{\boldsymbol{\theta}}(\boldsymbol{x}_i) = \frac{1}{B}\sum_{a=1}^{B} f_{\boldsymbol{\theta}}(T_a(\boldsymbol{x}_i))$ be the model average over all the B augmentations. We can show that we can express the bias as

$$\text{Bias}(\boldsymbol{\theta}) = \frac{1}{n}\sum_{c=1}^{C}\sum_{i \in N_c}\left\|\boldsymbol{e}_c - \bar{f}_{\boldsymbol{\theta}}(\boldsymbol{x}_i)\right\|^2.$$

Notice that as in a random labeling experiment, the number of classes C can be considered as a hyperparameter, hence if we choose $C >> n$, then each sample $\boldsymbol{x}_1, \dots, \boldsymbol{x}_n$ is assigned a different class with high probability. In this case, the "bad bias" given by assigning the same label to samples of different classes vanishes, and one has:

$$\text{Bias}(\boldsymbol{\theta}) = \frac{1}{n}\sum_{i=1}^{n}\left\|\boldsymbol{e}_i - \bar{f}_{\boldsymbol{\theta}}(\boldsymbol{x}_i)\right\|^2,$$

where w.l.o.g we have re-ordered the labels such that the i-th label is assigned to sample $\boldsymbol{x}_i$. In this limiting case, the bias term represents a contrastive term that encourages the average model $\bar{f}_{\boldsymbol{\theta}}(\boldsymbol{x}_i)$ to be different from the other samples $\boldsymbol{x}_j \neq \boldsymbol{x}_i$ and their augmentations. In this sense, this term can be related to contrastive SSL. On the other hand — unlike contrastive SSL — the distance between the average models of two datapoints cannot be arbitrarily large, and once the loss is driven to zero, $\text{Bias}(\boldsymbol{\theta}) = 0$ and it is trivial to see that $\left\|\bar{f}_{\boldsymbol{\theta}}(\boldsymbol{x}_i) - \bar{f}_{\boldsymbol{\theta}}(\boldsymbol{x}_j)\right\|^2 = 2$.
We refer the reader to Appendix B for experiments with varying number of classes. We observe that, as hypothesized, the influence of the bias diminishes and performance increases as a function of the number of classes C.

B More Experiments

In the following we present more empirical evidence that may help better interpret our findings.

Role of the Projector. We visualize in Fig. 7 the effect of varying the size of the hidden layer in the projector. There is a threshold under which learning is impossible (or at least very hard given a fixed computational budget). Surprisingly, using a larger projector seems beneficial beyond the point where we manage to decrease the loss significantly and achieve memorization of the original dataset.

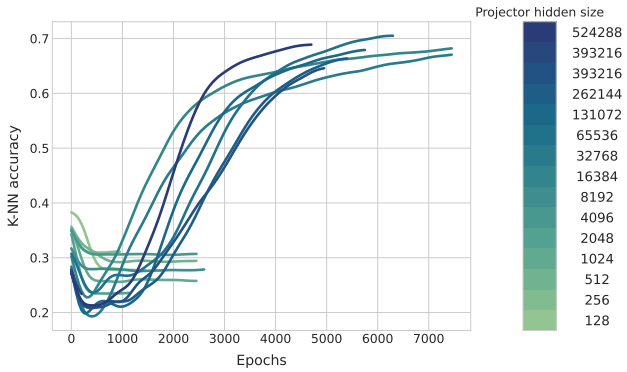

Figure 7: Nearest-neighbour probing accuracy as function of the size of the projector.

The role of the number of random classes. So far we assigned to each sample a random label in $\mathbb{R}^C$, where C is the number of classes in the original dataset. In principle, increasing the number of

classes, decreases the strength of the noise provided to the model. We verify this in Fig. 8, where we vary the number of possible classes each sample is randomly assigned to. In the extreme case, every sample is assigned its unique class label $\boldsymbol{y}_i = \boldsymbol{e}_i$, where $\boldsymbol{e}_i \in \mathbb{R}^n$, recovering the result of Dosovitskiy et al. (2014) which we refer to as 'Per sample'. We observe that with increasing number of classes, performance improves (as less noisy assignments are made). We refer the reader to Appendix A for a more formal connection.

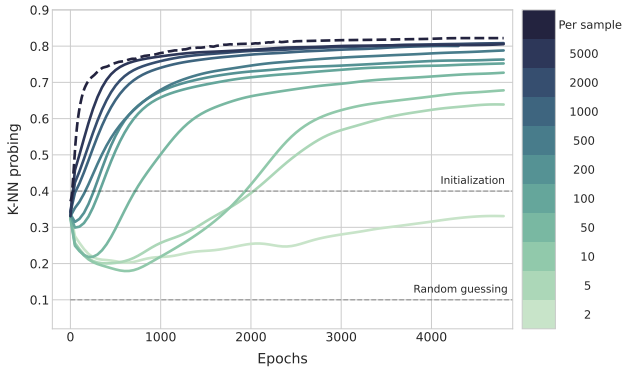

Figure 8: Nearest-neighbour probing accuracy as function of the number of classes.

Transferability. Features learnt with random labels are also useful when evaluated on different datasets. In Fig. 9 on the right-hand-side, we transfer the features learnt on *CIFAR10*, to *CIFAR100* and *STL10* (Coates et al., 2011). We observe that we can achieve strong downstream performance, highlighting the strength of the features learnable under random labels. Moroever, we see that using data augmentation is crucial when label noise is high as without data augmentation

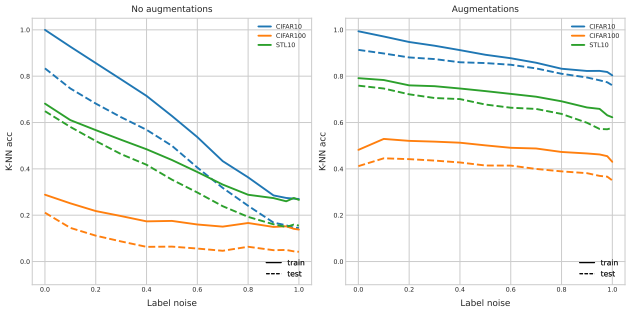

Figure 9: Nearest-neighbour probing accuracy for transfer learning to different datasets as a function of label noise. A *ResNet18* is trained based on random labels on *CIFAR10* with (right) and without (left) data augmentation.

Dependence on noise and speed of convergence. Augmentations have been shown to be especially useful under the presence of heavy label noise. In Fig. 10 we visualize the performance achieved during the first stage of training under varying level of label noise. Label noise specifies the percentage of labels that are randomly permuted versus the percentage of labels that are kept the same.

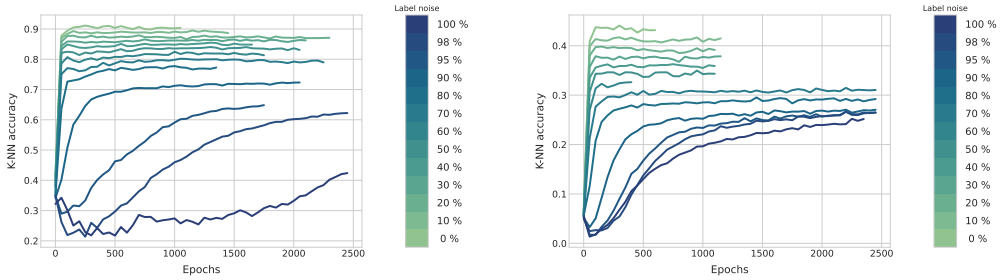

(a) *CIFAR10* (b) *TinyImageNet*

Figure 10: Nearest-neighbour probing during training for the *CIFAR10* and *TinyImageNet* datasets during training.

Effect on the strength of the augmentation. Although malign memorization gets impossible as the number of augmentations $B \to \infty$, the strength of the augmentations themselves plays a role on the generalization achieved. The strength of the augmentation basically dictates the strength of the invariance that the model has to learn, which also correlates with the quality of the features learned as seen in Fig. 11. To control strength we use strength level of RandAugment (Cubuk et al., 2020). We clearly see that stronger augmentations are beneficial for the quality of the embeddings, underlining the fact that invariance indeed plays a key role in benign memorization.

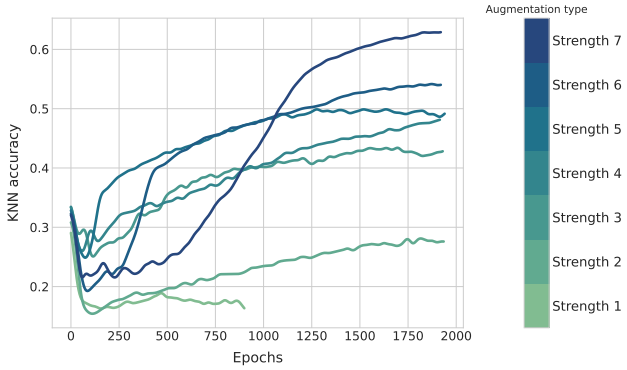

Figure 11: Nearest-neighbour probing accuracy when trained on random labels with varying strength of (infinite) augmentations.

Varying levels of label noise. Previous works have highlighted the importance of augmentations in the presence of high label noise. We examine the relationship between label noise and generalization both with and without augmentations in Fig. 12. We see that while data augmentation is not so crucial for clean labels, its role becomes more and more critical as we increase the amount of label noise. Without augmentations, we suffer from a strong decrease in performance, eventually ending with random guessing as we reach complete label noise. On the other hand, using augmentations stabilizes this decay and we still achieve strongly non-trivial performance even in the setting of complete label noise.

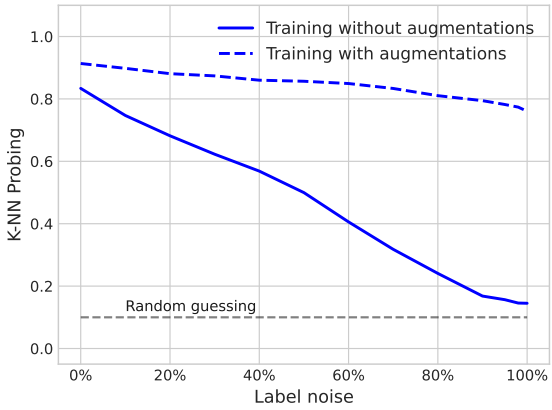

Figure 12: Nearest-neighbour probing accuracy when trained on varying levels of label noise with and without augmentations.

C TOY EXAMPLE

To better understand the role of augmentations with respect to the capacity of the model we devise a simple toy setting.

We consider samples $\boldsymbol{x_i}, \dots, \boldsymbol{x_n} \in \mathbb{R}^d$, that belong to one of the C underlying classes. We select the first $d_1 < d$ coordinates to denote the true class assignment z_i, uniformly selected from the set $\{1, \dots, C\}$, by sampling from a mixture of Gaussian distributions and let the rest $d - d_1$ dimensions correspond to noise. More specifically:

$$\boldsymbol{x_i}_{[:d_1]}|_{z_i=k} \sim \mathcal{N}(\boldsymbol{\mu}_i, \boldsymbol{\Sigma_1}),$$
$$\boldsymbol{x_i}_{[d_1:]} \sim \mathcal{N}(\boldsymbol{0}, \boldsymbol{\Sigma_2}).$$

With $\boldsymbol{\mu}_i$ we denote the cluster centers that are sampled randomly. In this case we consider augmentations of the samples:

$$\bar{\boldsymbol{x}} = \boldsymbol{x} + \boldsymbol{a},$$
$$\text{where } \boldsymbol{a}_{[:d_1]} = \boldsymbol{0}$$
$$\text{and } \boldsymbol{a}_{[d_1:]} \sim \mathcal{N}(\boldsymbol{0}, \boldsymbol{\Sigma_3}).$$

As set the covariance matrices as $\Sigma_3 = \Sigma_2 = 10\,\Sigma_1 = \sigma^2 \boldsymbol{I}$, where $\boldsymbol{I}$ is the identity matrix. It is obvious that learning invariance for this task under these augmentations leads to embeddings that ignore the noise subspace. We employ is this case a simple linear encoder $h_{\boldsymbol{W}}(\boldsymbol{x}) = \boldsymbol{W}\boldsymbol{x}$, with $\boldsymbol{W} \in \mathbb{R}^{d \times d}$.

As a projector we use $g_{\boldsymbol{V}}(\boldsymbol{x}) = \sum_{i=1}^{K} \frac{\frac{1}{\|\boldsymbol{x} - \boldsymbol{v_i}\|}}{\sum_{j=1}^{K} \frac{1}{\|\boldsymbol{x} - \boldsymbol{v_j}\|}} \boldsymbol{l}_i$. Here $\boldsymbol{l_i}$ is a one hot encoding sampled randomly from the set $\{\boldsymbol{e}_1, \dots, \boldsymbol{e}_C\}$. We choose such a projector as it is not difficult to verify that for $K >= d$ the capacity of the model, in this case, will be approximately fixed to the number of K patterns that we compare the embedding space against. Additionally, its non-linear nature guarantees that any possible invariance learning will occur at the encoder instead. In Fig. 13 we visualize the K-NN probing for the downstream task of correctly predicting the clean label of unseen test samples, after training on random labels. By varying the number of samples n and augmentations B available, we directly control whether full memorization can take place or not. When the number of samples n is smaller than $\frac{\mathcal{C}}{B}$, where $\mathcal{C}$ is the capacity of the model, full memorization is possible, which discourages any feature learning, leading to bad generalization.

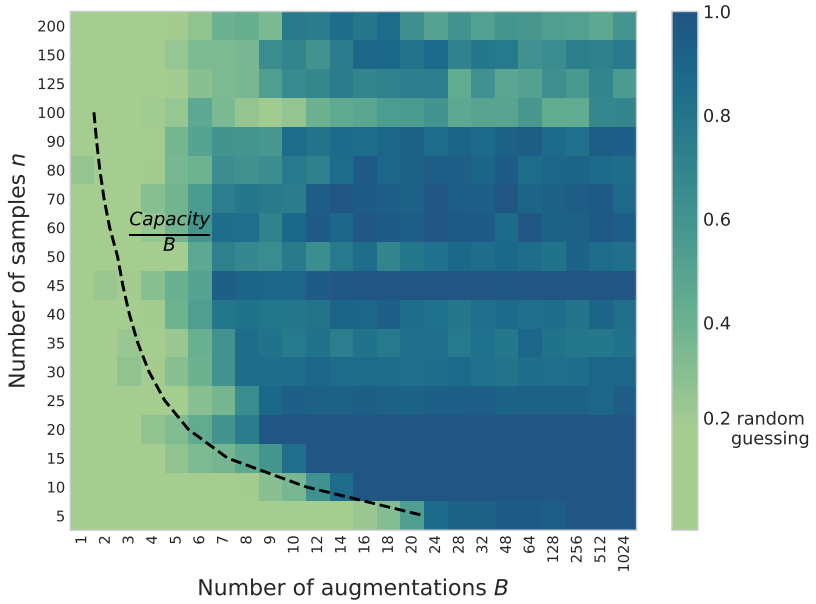

Figure 13: K-NN probing for the downstream class assignment on unseen test points for the toy example, after training on random labels.

D Experimental Setup

As commonly done for smaller size images (Chen & He, 2021; Hua et al., 2021a), we use a variant of the *ResNet18* architecture, where the max-pooling layer is removed, and the first convolution is modified to have a kernel size of 3 and a stride of 1. We also remove the last fully connected layer, as we replace it with our projector. We provide more details about the hyperparameters used in Table 4. For the experiments on *TinyImageNet*, we rescale images to a size of 64×64 and additionally restore the stride of the first convolution to the value 2. We apply the same modification to VGG when trained on *TinyImageNet*.

	Hyperparameters	Value
Augmentations	Random cropping scale	(0.08, 1)
	Horizontal flip probability	0.5
	Color-Jittering	(0.8, 0.8, 0.8, 0.2)
	Grayscale probability	0.2
	Mixup	yes
Parameters	image-size	32/64
	clip-norm	'none'
	dropout	'none'
	Projector size	65536
	Projector MLP normalization	'none'
Training	Learning rate	$4\epsilon^{-3}$
	Learning rate scheduler	'none'
	Adam (β_1, β_2)	(0.9, 0.999)
	Batch size	256
	Weight decay	0.0
	Loss	'mse-loss'

Table 4: Hyperparameters for the random labels experiments.